crystallographic directions while the orientation of the third crystal axis naturally arises from the two directions imposed and from the internal crystal symmetry (Fig. 1b).

Osuji and colleagues sandwich the sample in between two parallel plates 10 μm apart. The flat disc-like molecules tend to align parallel to the flat walls. For the liquid-crystalline phase with long-range orientational order, the molecular alignment at the surface defines the orientation of the columns through the whole sample thickness. However, the lateral orientation of the hexagonal columnar network is still random. To remove this ambiguity, the authors apply a magnetic field along the film, which aligns the flat TDIB cores parallel to the field direction. This condition is automatically fulfilled in the non-tilted columnar phase and the magnetic field does not provide any lateral alignment of the structure. However, at a temperature below 58 °C the tilt defines a unique direction that minimizes the magnetic interaction energy (Fig. 1a). By slowly cooling the sample in the magnetic field, it is possible to obtain high-quality single-crystal films where the hexagonally arranged columns are separated by as little as 4.12 nm. In contrast to hard matter, here the alignment can be performed after casting, which can be advantageous for technological processing. Despite the fact that self-organized soft matter systems are prone to various defects[5], the alignment treatment leads to very high-quality periodic positional order with nanometre precision (Fig. 1c).

Applications of this approach can be envisioned, for example, in magnetic recording. The hexagonal nanostructure can be fixed in position on light irradiation and readily used as a template. The molecule cores could be etched away and filled with a magnetic material. In this way, materials with 7×10^{12} magnetic nanocylinders per square centimetre can be obtained where the diameter and length of each nanocylinder can be controlled by the chemical etching process. Using the magnetization state of each nanoparticle as one bit of information, an information density of more than 40 Tbit per square inch is easily reached, which is an order of magnitude higher than the current state of the art[6,7]. The next challenge would consist of developing a technology that allows for the modification and reading of the magnetization states of the individual particles. Alternatively, the single crystals described by Osuji and colleagues could be subjected to selective etching to remove the TABA tails while leaving the TDIB core intact to create a template for a honeycomb nanostructure with massless electrons[8]. In addition, the use of non-collinear fields during or after the crystal growth could also prove useful for other applications such as protein crystallography[9]. ❐

Andrei V. Petukhov[1,2]
[1]*Van 't Hoff Laboratory for Physical and Colloid Chemistry, Debye Institute for Nanomaterials Science, Utrecht University, Utrecht, the Netherlands.*
[2]*Laboratory of Physical Chemistry, Eindhoven University of Technology, Eindhoven, the Netherlands.*
e-mail: a.v.petukhov@uu.nl

Published online: 23 October 2019
https://doi.org/10.1038/s41563-019-0517-y

References
1. Feng, X. et al. *Nat. Mater.* https://doi.org/10.1038/s41563-019-0389-1 (2019).
2. Czochralski, J. *Z. Phys. Chem.* **92**, 219–221 (1917).
3. Nickmans, K. & Schenning, A. P. H. J. *Adv. Mater.* **30**, 1703713 (2018).
4. Frank, F. C. & Chandrasekhar, S. *J. Phys. Fr.* **41**, 1285–1288 (1980).
5. Forster, S. et al. *Nat. Mater.* **6**, 888–893 (2007).
6. Mallary, M., Torabi, A. & Benakli, M. *IEEE Trans. Magn.* **38**, 1719–1724 (2002).
7. Pi, S. et al. *Nat. Nanotechnol.* **14**, 35–39 (2019).
8. Boneschanscher, M. P. et al. *Science* **344**, 1377–1380 (2014).
9. Wakayama, N. I. *Cryst. Growth Des.* **3**, 17–24 (2003).

PLASMONICS

Lasing under ultralow pumping

Ultralow-threshold plasmonic lasers under continuous-wave pumping at room temperature have been created using lattice plasmonic cavities integrated with gain material consisting of upconverting nanoparticles.

Ren-Min Ma

Threshold is one of the most important figures of merit for laser devices. It characterizes the minimum pump power for the onset of lasing emission (Fig. 1a). Threshold power consists of two major parts, one for achieving population inversion of the gain material (that is, to make the gain medium transparent), and the other for compensating the cavity loss. In the past decade, plasmonic nanolasers emerged as a new class of lasers with great potential for shrinking the size of integrated photonic circuits to be comparable to modern electronic devices[1–4]. In order to realize such an unprecedented miniaturization, part of the light energy of a plasmonic nanolaser has to be stored in the form of free-electron oscillation inside the metal. However, free-electron oscillation dissipates energy to heat rapidly; this additional metallic loss has led so far to plasmonic nanolasers with high lasing thresholds. Writing in *Nature Materials*, P. James Schuck, Teri W. Odom and colleagues[5] have now achieved a record low threshold of 70 W cm^{-2} in plasmonic lasers under continuous-wave pumping at room temperature, which is about two orders of magnitude lower than commercialized laser diodes.

Because the stimulated emission needs to dominate in the lasing state, laser threshold can be unambiguously defined as the condition in which the rates of spontaneous and stimulated emission into the laser mode are equal (Fig. 1b). According to Einstein's 1917 paper on spontaneous emission and stimulated emission coefficients, this condition is equivalent to saying that a lasing mode should contain one photon to reach the threshold[6]. Hence for a given cavity loss, the minimum power to maintain a photon in the laser mode requires a power (P_{Cavity}) of $\gamma_{\mathrm{C}} \times h\nu \times \frac{1}{\beta}$, where γ_{C} is the cavity photon loss rate, $h\nu$ is the energy of the one photon, and β is the spontaneous emission factor, the fraction of spontaneous emission directed into the laser mode. In a conventional laser, the photon loss rate can be significantly suppressed by cavity feedback optimization. However, in a plasmonic laser cavity, the photon loss rate usually reaches 10^{13}–10^{14} s^{-1} due to the parasitic metallic loss. Assuming an emitted photon energy $h\nu$ of ~1 eV and a β factor of 1, we can obtain a minimum threshold power of plasmonic nanolasers around 1–10 μW. This may not sound like a very high power but given the very small

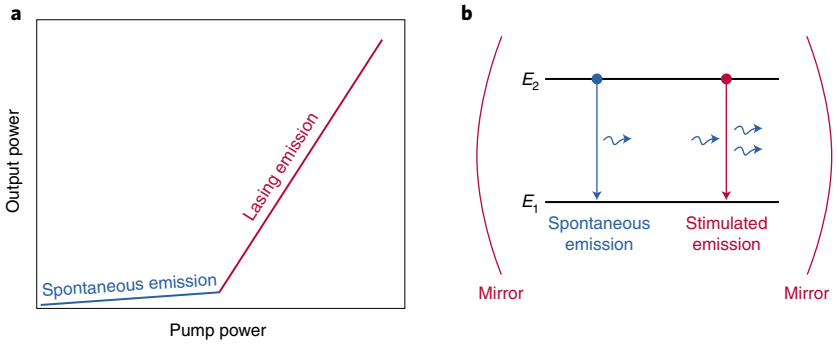

Fig. 1 | Threshold of lasers. a, Threshold characterizes the minimum pump power for the onset of lasing emission from spontaneous emission. In conventional lasers, it appears as a kink in the light–light curve in linear scale. **b**, Laser threshold can be unambiguously defined as the condition in which the rates of spontaneous and stimulated emission into the laser mode are equal. According to Einstein's 1917 paper on spontaneous emission and stimulated emission coefficients, this condition requires one photon maintained in the laser mode.

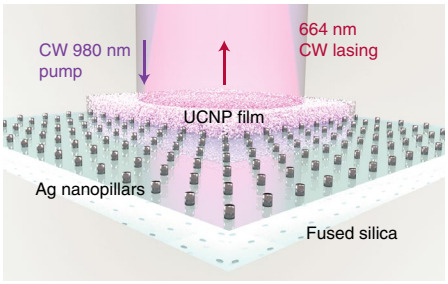

Fig. 2 | Ultralow-threshold plasmonic lasers under continuous-wave (CW) pumping at room temperature. These have been created using lattice plasmonic cavities integrated with gain material consisting of upconverting nanoparticles (UCNPs). Compared to a single plasmonic nanoparticle cavity, the lattice one has a higher quality factor due to the suppression of radiative loss, while maintaining the subwavelength localized fields around each nanoparticle. Because only a single photon is required in the lasing mode at threshold, this collective lattice mode dramatically lowers the threshold power density. Together with UCNPs with very long spontaneous emission lifetime to lower the power for achieving population inversion, these lattice plasmonic lasers have an ultralow threshold around 70 W cm^{-2}. Adapted from ref. [5], Springer Nature Ltd.

foot print (down to a few tens of nanometres in diameter) of plasmonic nanolasers, the threshold power density could reach the order of MW cm^{-2}, which is about two orders of magnitude higher than the commercialized semiconductor laser diode[7].

The total threshold power should also include the power needed to pump and maintain the carriers at an upper energy level for population inversion. The minimum power to maintain population inversion requires a power (P_{Gain}) of $\gamma_{SP}\times E_{21}\times V\times n_{tr}$, where γ_{SP} is the spontaneous emission rate, E_{21} is the energy required to pump carriers onto excited energy level ($\sim h\upsilon$), V and n_{tr} are the physical volume and the transparency carrier density of the gain material. For normal semiconductor gain materials, γ_{SP} and n_{tr} are on the order of ~10^9 s^{-1} and ~10^{17}–10^{18} cm^{-3} respectively.

In their work, Schuck, Odom and co-authors realized plasmonic laser device with extremely low threshold via a unique combination of lattice plasmonic cavity and a special type of upconverting nanoparticle gain material, both of which play an important role in the reduction of threshold power density (Fig. 2). The lattice plasmonic cavity consists of a metal nanoparticle array, in which each small metal nanoparticle can be treated as a dipole emitter, whereas interference of dipolar radiation introduces a sharp collective lattice resonance mode with directional emission[8–10]. Compared to a single plasmonic nanoparticle cavity, the lattice plasmonic cavity has a higher quality factor due to the suppression of radiative loss, while maintaining the subwavelength localized fields around each nanoparticle. The cavity has an enlarged mode volume and physical footprint determined by the whole lattice size. Because only a single photon is required in the lasing mode at threshold, this collective lattice mode dramatically lowers the threshold power density required for plasmonic mode lasing.

To further reduce the lasing threshold, the authors used lanthanide-based upconverting nanoparticles (UCNPs) as the gain medium. UCNPs are photostable solid-state nonlinear emitters that can efficiently absorb multiple near-infrared photons and emit at shorter wavelengths[11]. In contrast to other conventional gain materials, UCNPs exhibit very long spontaneous emission lifetimes (typically hundreds of μs), which leads to low saturation intensities that could facilitate continuous-wave pumping and population inversion build-up. Moreover, they exploited core-shell UCNPs with high Ln content to improve the emission property, which resulted in even further reduced saturation intensities for lowering the lasing threshold[12]. Importantly, the lattice plasmon resonance is tuned to spectrally overlap with designed UCNPs emission wavelength to enhance their coupling, and to lower the upconverting lasing thresholds for improving the device stability under continuous-wave pumping.

The ultralow-threshold plasmonic laser under continuous-wave pumping at room temperature presented here represents a major step towards practical applications of nanoscale photonic devices. More importantly, it proves unambiguously that plasmonic lasers are not intrinsically linked with high-threshold power density, which endorses the exploration of plasmonic lasers in various practical applications. The next critical step would be to increase the external quantum efficiency of the current device. It will also be interesting to see the demonstration of semiconductor-based lattice plasmonic lasers operating under electrical pumping and showing faster modulation speed. ❐

Ren-Min Ma[1,2]
[1]*School of Physics, Peking University, Beijing, China.*
[2]*State Key Lab for Mesoscopic Physics, Peking University, Beijing, China.*
e-mail: renminma@pku.edu.cn

Published online: 23 October 2019
https://doi.org/10.1038/s41563-019-0513-2

References

1. Bergman, D. J. & Stockman, M. I. *Phys. Rev. Lett.* **90**, 027402 (2003).
2. Berini, P. & De Leon, I. *Nat. Photon.* **6**, 16–24 (2012).
3. Wang, S. et al. *Nat. Commun.* **8**, 1889 (2017).
4. Ma, R.-M. & Oulton, R. F. *Nat. Nanotechnol.* **14**, 12–22 (2019).
5. Fernandez-Bravo, A. et al. *Nat. Mater.* https://doi.org/10.1038/s41563-019-0482-5 (2019).
6. Einstein, A. *Phy. Z.* **18**, 121–128 (1917).
7. Khurgin, J. B. & Sun, G. *Nat. Photon.* **8**, 468–473 (2014).
8. Ross, M. B., Mirkin, C. A. & Schatz, G. C. *J. Phys. Chem. C.* **120**, 816–830 (2016).
9. Zheludev, N. I., Prosvirnin, S. L., Papasimakis, N. & Fedotov, V. A. *Nat. Photon.* **2**, 351–354 (2008).
10. Zhou, W. et al. *Nat. Nanotech.* **8**, 506–511 (2013).
11. Zhou, B., Shi, B., Jin, D. & Liu, X. *Nat. Nanotechnol.* **10**, 924–936 (2015).
12. Tian, B. et al. *Nat. Commun.* **9**, 3082 (2018).